Pediatr Radiol (2013) 43:393–405
DOI 10.1007/s00247-012-2610-0

MINISYMPOSIUM

Evaluation of bone viability

Isabel Roca · Ignasi Barber · Cesar G. Fontecha · Francisco Soldado

Received: 24 June 2012 / Revised: 9 September 2012 / Accepted: 16 October 2012

Abstract Bone scintigraphy is an excellent tool to assess bone viability. The functional information provided is crucial in several clinical settings, like the detection of avascular necrosis, septic embolism, frostbite lesions and osteonecrosis, and to evaluate the results of surgical treatment in cases of avascular necrosis. Mechanisms to obtain molecular images, as well as different kind of techniques, are detailed. Comparative and multimodality imaging to focus on any clinical problem and a review of the clinical indications reflect the multidisciplinary approach with close collaboration between orthopaedists, radiologists and nuclear medicine physicians. Finally, an effort has been made to list the most important points of imaging of bone viability in children.

Keywords Bone viability · Scintigraphy · SPECT · Children

I. Roca (✉)
Nuclear Medicine Service, Hospital Universitari Vall Hebron,
Passeig Vall Hebron 119,
08035 Barcelona, Spain
e-mail: iroca@vhebron.net

I. Barber
Paediatric Radiology Department, Hospital Universitari Vall Hebron, Barcelona, Spain

C. G. Fontecha · F. Soldado
Paediatric Orthopaedic Unit, Hospital Universitari Vall Hebron, Barcelona, Spain

F. Soldado
Pediatric Upper Extremity Surgery and Microsurgery, ESSAUDE Lisbon (Hospital da Luz/Beatriz Angelo), Lisbon, Portugal

Introduction

A good blood supply and a normal osteoblastic/osteoclastic activity underlie bone viability. Evaluation of bone viability is challenging in several clinical settings: detection of avascular necrosis, septic embolism, frostbite lesions, burns and osteonecrosis. It is also crucial to evaluate the results of surgical treatment of avascular necrosis. Bone scintigraphy is an excellent tool to assess bone viability.

The use of scintigraphy in the assessment of bone is based on its increased sensitivity in detecting abnormalities over other imaging techniques and its ability to survey the entire skeleton, at reasonable cost.

Bone scintigraphy performed after injecting ^{99m}Tc-diphosphonates or ^{18}F-fluoride, with planar, pin-hole, SPECT, SPECT-CT or PET-CT images, should always be interpreted in close correlation with history and clinical findings, and in conjunction with other imaging techniques, including radiography, CT and MRI. Overall interpretation of molecular and anatomical images, in the clinical setting, will allow us to reach the best diagnostic accuracy.

Indications for bone viability evaluation with bone scintigraphy were introduced in the 1960s for the assessment of skeletal trauma, including bone healing, non-union and early detection of bone fragment necrosis [1, 2]. In the 1970s, bone scintigraphy was successfully used to establish the limit of viable bone in the frostbite injuries of the extremities [3]. Several other papers have been published on the same topic since then [4–7]). The utility of bone scintigraphy has also been reported in the evaluation of bone necrosis extension after severe electric burns [8, 9].

In cases of avascular necrosis and osteochondrosis, like Legg-Calvé-Perthes disease, bone scintigraphy has a relevant role and a definite impact on the clinical management, providing early detection and prognostic information [10].

The value of bone scintigraphy to evaluate bone graft uptake after surgery has also been reported [11, 12].

In cases of bone and joint infection, focal decreased bone uptake can be detected. This is especially relevant in hip arthritis, in which a "cold" hypoperfused femoral head in scintigraphy may reflect an interruption of the blood supply to the epiphysis, an increased intra-articular pressure, bone marrow oedema or bone necrosis [13]. Meningococcal septicaemia is another cause of septic bone infarct, and bone scan has demonstrated to change the therapeutic management by showing the existence of necrotic areas within the bone [5].

Growth plate activity can also be assessed by bone scintigraphy. Total or partial hypoactivities represent a total or a segmental closure due to trauma or infection [14]. Surgery is successful to correct early plate closure and inadequate leg length. If a surgical treatment is planned, MRI offers high anatomical evaluation, and bone scintigraphy provides physiological information about the growth activity.

Molecular bone imaging: mechanisms

The imaging basis of bone scintigraphy is the high affinity between ^{99m}Tc-labelled phosphonates and hydroxiapatite crystals, and the incorporation of this complex to viable bones on the basis of a good vascular supply and osteoblast activity [8, 11, 12]. ^{18}F-fluoride also labels the hydroxyapatite and has a similar uptake mechanism as ^{99m}Tc, reflecting regional blood flow and new bone formation. Fluorine-18 has been used since the 1960s and 1970s, but with development of PET imaging it has shown a renaissance for skeletal imaging, offering a much higher image resolution compared with conventional bone scintigraphy. Thus, we expect an expansion in its use in the near future [10, 13, 15–17].

The absolute skeleton uptake of both tracers is approximately 50%; the bone uptake is rapid and the background activity tends to decrease quickly due to urinary excretion. Bone tissue is continuously regenerating, with osteoblastic activity (bone formation) and osteoclastic activity (bone resorption).

Skeletal metabolism changes according to physiological and pathological conditions and bone scintigraphy is sensitive to these changes [8, 12]. In healthy children, growth plate metabolism and, subsequently, bone uptake in bone scintigraphy is much higher than diaphyseal or epiphyseal uptake, decreasing during sickness or when the child is bedridden, and recovering quickly when the child returns to normal activity.

Molecular bone imaging: types

A variety of images can be obtained, including planar (whole-body or spot frames), pinhole, SPECT, SPECT-CT, PET and PET-CT images. When evaluating bone viability, planar bone scan images are well established as the standard of reference. In select indications, the use of SPECT and SPECT-CT increases diagnosis accuracy and permits a more precise anatomical localisation of the lesion [18, 19].

Vascular images

When a three-phase bone scan is performed, the vascular phase should be obtained 30–60 s after the IV tracer injection. This phase will help detect focal or diffuse hyperaemia, differentiating between arterial and venous compounds, and it is essential for the detection of inflammatory changes. In children, the blood pool images should be obtained as soon as possible after the IV injection, and always before the first 3-4 min after injection of the tracer. Bone uptake due to rapid bone metabolism in children promptly masks the blood pool activity.

Planar bone images

Planar bone images continue to be the standard of reference in bone scintigraphy imaging. Image resolution is the cornerstone for children. Higher resolution is obtained with spot frames rather than whole-body images, with the child close to the collimator and avoiding movements during acquisition. Positioning the child close to the collimator will increase image resolution and decrease acquisition time.

Pinhole images

Pinhole images are the highest-resolution images that can be produced with a gamma camera. By magnifying the area of interest with a pinhole collimator, we can reach even higher resolution than with conventional planar or SPECT images. The limitations are the unavailability of this kind of collimator, the amount of time the process takes and the immobilisation required to obtain high-resolution images (5–10 min). Positioning of the child, evaluation of small lesions or lesions located in small peripheral joints are also limitations for the use of pinhole imaging.

SPECT and SPECT-CT

With the new hybrid gamma cameras, SPECT and SPECT-CT are replacing pinhole images, having an emerging role in bone imaging [20].

SPECT is complementary to planar images. Due to its higher sensitivity in detecting vertebral lesions, it is mandatory in cases of back pain even when the planar images show no abnormal uptake.

SPECT-CT allows the fusion of the functional SPECT frames with the CT anatomical images. Although a low-dose

CT is mandatory, the use of this hybrid technique in paediatrics should be strictly limited, given its radiation burden. Fusion of SPECT images with diagnostic CT or MRI images is also possible and helpful, allowing a precise anatomical localisation of an abnormal uptake without additional radiation.

Limitations of SPECT-CT are the time of acquisition (15 min, which may require sedation in children) and the CT radiation dose. In bone viability studies, the added value of SPECT-CT images is crucial for the anatomical location before and after surgery of cold areas and bone uptake in vascularised grafts.

PET-CT

^{18}F-FDG imaging has a much higher anatomical resolution and a higher sensitivity for the detection of bone lesions than conventional bone scintigraphy (Fig. 1). In addition, fused PET-CT images offer a nice correlation of metabolic and anatomical information. But we should keep in mind that it is not widely available and it has much higher costs than bone scintigraphy. The dosimetry of bone scintigraphy and ^{18}F-PET are directly related to the injected dose of tracer. For a 5-year-old child weighing 18 kg, following the Society of Nuclear Medicine (SNM) recommendations, the whole-body dosimetry related to ^{18}F-PET is not significantly higher than the one related to bone scintigraphy [21]. On the other hand, following the European Association of Nuclear Medicine (EANM) dosage card recommendations, with much higher ^{18}F recommended doses, the whole-body effective dose is 38% higher for ^{18}F [22–24]. The organs with largest radiation absorbed dose differ in both techniques, being the bladder in ^{18}F and the bone surface in conventional bone scintigraphy.

When comparing the whole-body effective dose using the SNM guideline [21] the recommended radiotracer dose of ^{18}F (2.22 MBq/kg) whole-body effective dose (in mGy, ^{18}F injected dose 2.22 MBq/kg) is 9% higher using the lowest ^{99m}Tc-MDP recommended dose (7 MBq/kg) and 31% lower with the highest ^{99m}Tc-MDP dose (11 MBq/kg).

With the development of new equipment, the recommended ^{18}F doses are decreasing, therefore radiation dose of ^{18}F-PET will decrease in the future and that is essential for its use in children.

Clinical indications

Avascular necrosis: bone infarcts

Osteonecrosis is a pathological process in which the compromise of bone vasculature leads to the death of bone cells and ultimate mechanical failure.

Non-traumatic avascular osteonecrosis is a well-reported complication of corticosteroid treatment for immunological and malignant diseases in children (Fig. 2). In epiphyseal areas, where there is a terminal vascular supply, the extent of the necrotic area is related to joint collapse and further degenerative changes.

Because osteonecrosis is often asymptomatic until late in the process, imaging is critical for its detection and characterisation in an early phase when interventions may be most

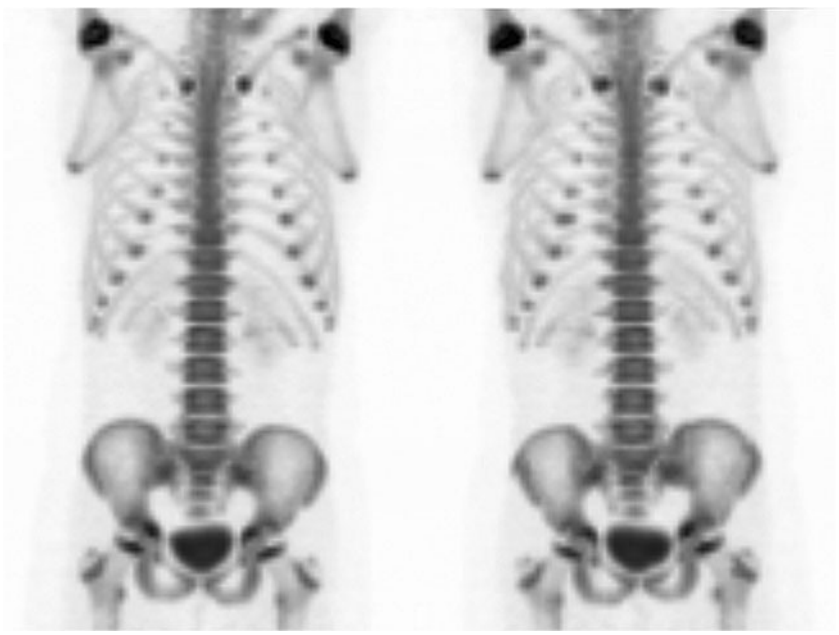

Fig. 1 Normal ^{18}F-PET in a 15-year-old patient. Images have similar bone pattern uptake, but much better resolution, higher bone/soft tissue ratio and the study is shorter than ^{99m}Tc-methylene diphosphonate (MDP) bone scintigraphy. (Case courtesy of Dr. Ted Treves, Children's Hospital Boston, Harvard Medical School, Boston, MA, USA)

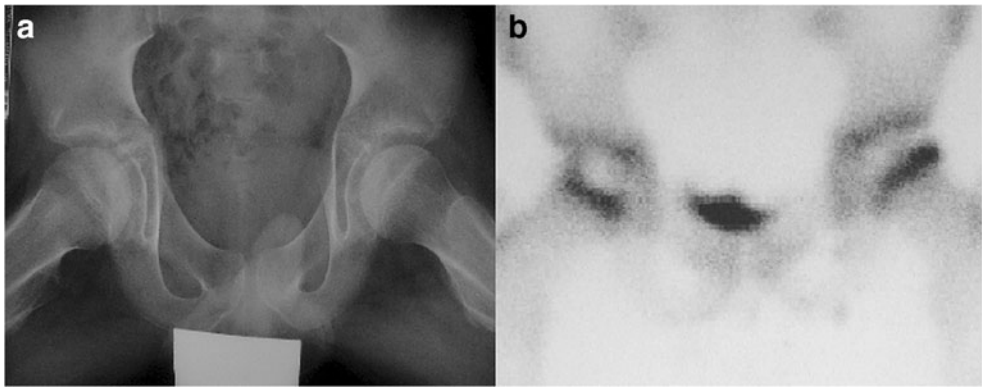

Fig. 2 Bilateral hip pain in a child with high-dose steroid treatment for idiopathic juvenile arthritis. **a** A radiograph (axial view) shows a slight sclerosis of both proximal femoral epiphyses without femoral head collapse. **b** Bone scintigraphy, planar image of both hips, shows cold areas on both femoral heads with more severe involvement on the left side. Findings are consistent with bilateral femoral head osteonecrosis stage IIa on the Ficat classification

effective to ameliorate its progression. MRI and SPECT are highly sensitive (MRI 85–100%, SPECT 85–97%) in the early diagnosis of avascular necrosis of the femoral head and in the study of the extent of the necrotic area [25]. Although MRI is relatively easy to perform and interpret, SPECT is more available worldwide.

One of the main advantages of bone scintigraphy in the evaluation of avascular necrosis is whole-body coverage. When the diagnosis of avascular necrosis in children is suspected and plain radiographs do not point to a specific area of involvement, bone scintigraphy may have a significant role as a primary tool being useful for the early diagnosis of suspected or unsuspected avascular necrosis [26].

Osteochondritis dissecans (OCD) is characterised by the necrosis of a fragment of subchondral bone that can progress to detachment of the cartilage and bone fragment (instability). Currently, X-ray and MRI are the imaging modalities of choice, but bone scan has also been used when radiographs are equivocal and could be useful when MRI is contra-indicated. A scintigraphic classification in four stages has been proposed and correlated with radiographs, symptoms and stability of the lesion, with a prognostic value [27].

Trauma is another cause of avascular necrosis. Bone scan has demonstrated to have an excellent sensitivity and predictive value for detection of avascular necrosis after surgical treatment of slipped capital femoris in children [28].

Early bone scintigraphy abnormalities demonstrated as photopenic area can predate radiographic changes by 4–6 weeks [29]. The development of new surgical approaches using vascularised bone grafts as a treatment to revitalise necrotic bone areas has created the need for an imaging tool to evaluate bone viability for both graft and host. SPECT-CT has been used for this purpose. The head of the femur is the most frequent area involved by avascular necrosis, and free vascularised fibular graft has been used to provide both vascular and mechanical supply to the necrotic bone. In patients treated for hip avascular necrosis with vascularised fibular graft, SPECT-CT performed 6 weeks after the surgical procedure has shown progressive tracer intake in the femoral head, suggesting graft viability and new bone formation within the necrotic area. Further follow-up and research is mandatory to evaluate its prognostic value. SPECT-CT may also be useful in the postsurgical evaluation of avascular necrosis in other anatomical regions.

Legg-Calvé-Perthes disease

Legg-Calvé-Perthes disease is characterised by ischaemic necrosis of the growing femoral head, followed by a reparative process. Although children younger than 5 years have a good prognosis, only 50% of older patients have reparative success. The extent of the necrosis is a prognostic factor. Complete epiphysis involvement or involvement of the lateral pillar are worrisome signs.

Basic imaging of the disease is based on plain radiographs, but it lacks the sensitivity and specificity needed to demonstrate vascular changes within the femoral head. Bone scintigraphy is highly sensitive and specific for detecting hypoperfusion of the femoral head in the avascular phase of the disease (Fig. 3). The best scintigraphical technique is to use pinhole magnification and to image in the frogleg lateral projection. The sensitivity and specificity of bone scintigraphy has been reported to exceed 95% when evaluating femoral head viability. Bone scintigraphy is also useful in the evaluation of the revascularisation phase as healing occurs. Conway [13] described two different scintigraphical revascularisation patterns of the ischaemic area in Legg-Calvé-Perthes disease. One is related to rapid recanalisation of existing vessels and the other is related to a

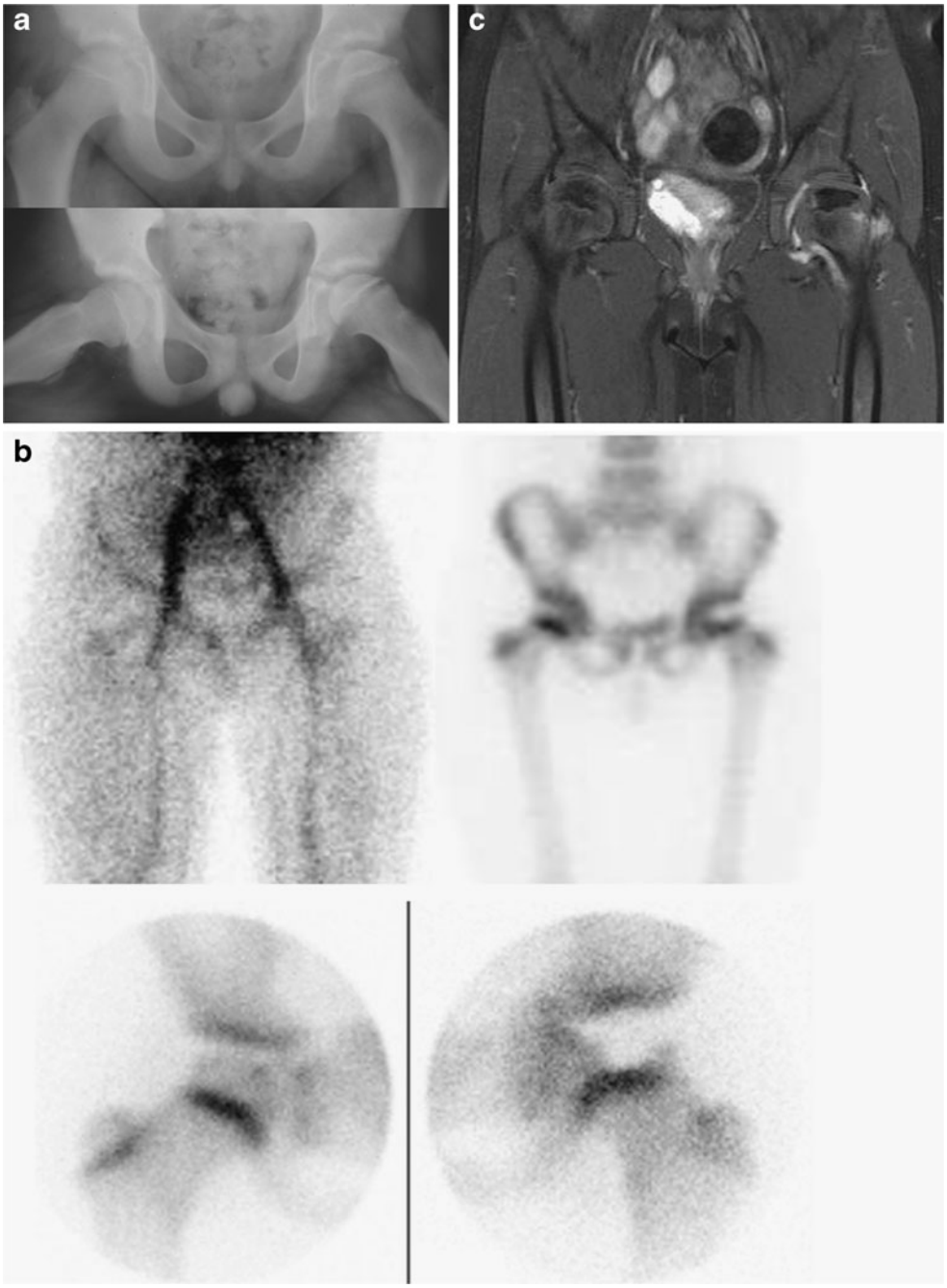

Fig. 3 Legg-Calvé-Perthes in a 4-year-old boy with a left limp, limited motion of the left hip and normal laboratory findings. **a** On radiographs, both hips show an abnormal left femoral head with slight sclerosis and loss of height. **b** Bone scan detects mildly increased blood pool on the left hip and a cold area on most the femoral head, with a perfused external pillar. Growth plate activity seems to be decreased (planar image). These findings are consistent with Legg-Calvé-Perthes disease. **c** On MRI, a coronal T1-weighted image after gadolinium enhancement shows asymmetry between both femoral heads with a slight collapse and decreased enhancement on the left side. Enhancement on the medial part of the femoral head and on the lateral aspect of the metaphysis suggests incipient revascularisation

sustained newly developed vessel neovascularisation. According to the Conway patterns, changes on bone scintigraphy and pinhole imaging precede the radiographic changes, and have an early prognostic value, correlating with later radiographic Catterall and Herring classifications [30, 31].

Complete involvement of the epiphysis is followed by a poor outcome, with flattening of the femoral head and early hip degenerative problems. SPECT-CT and pinhole imaging can detect the degree of involvement and are useful prognostic tools.

The main limitations of bone scintigraphy in Legg-Calvé-Perthes disease are the radiation risk and the lack of morphological detail of the femur head and its relationship with acetabular fibrocartilage.

As new surgical procedures are developed to restore epiphyseal blood perfusion, such as surgical forage through the physis, new indications for bone viability evaluation arise. Bone scintigraphy is useful in the evaluation of reperfusion and, even more important, in the evaluation of bone regeneration within the necrotic area after surgical intervention.

The use of MRI in Legg-Calvé-Perthes disease is still under debate, but it has been proposed as a non-ionising substitute for bone scintigraphy [32]. The most important MRI prognostic signs include the extent of femoral capital epiphysis involvement, the degree of metaphyseal changes and the lateral subluxation of the femoral head. In the future, the use of advanced MRI, including diffusion/perfusion imaging and dynamic contrast enhancement, may play an important role in the evaluation of Legg-Calvé-Perthes disease [21, 32–34].

Sickle cell anaemia

Classic characteristic features of sickle cell anaemia in bone scintigraphy are related to the expansion of haematopoietic bone marrow through the skeleton. Bone marrow infarction is a significant complication of sickle cell disease. The appearances of infarction at scintigraphy with ^{99m}Tc-MDP vary with time. Detection of cold areas within the bone marrow is challenging. Bone scintigraphy has a higher sensitivity during the revascularisation phase in which areas of increased bone uptake are evident.

Bone marrow infarction can be depicted using ^{99m}Tc-sulphur colloid (bone marrow scans), but it lacks specificity distinguishing acute from chronic changes.

The most relevant diagnostic dilemma in these patients is the high prevalence of superimposed osteomyelitis. In this clinical context, bone scintigraphy offers the advantage of whole-skeleton imaging and the accuracy of dynamic triple phase ^{99m}Tc-MDP (Fig. 4). MRI is also sensitive in the early phase of bone marrow infarction and may be useful in the diagnosis of superimposed osteomyelitis with an important role demonstrating soft-tissue fluid collections [35].

Bone infection

Bone infection can usually be diagnosed with 90% accuracy using a three-phase ^{99m}Tc-MDP bone study but is non-specific, as an increase in uptake identifies an area of increased bone-mineral turnover, not infection per se.

Some cold images can be seen in some circumstances that are not bone necrosis (Fig. 5). In virulent onset of the disease with high fever and severe bone pain, the bone scan can show cold bone lesions with decreased uptake on the initial imaging study delayed views, being positive at the end of the first week; this is believed to result from interruption of blood supply caused by increased local pressure (Fig. 6). Also, transient photopenic joint can occur due to the inability of the radiopharmaceutical to reach the site of the infection if there is a high joint pressure in cases of great joint effusion [36]. Nuclear medicine can play a role in the assessment of complications of bone infection. Confirmation of an area of isolated and necrotic bone can confirm the diagnosis of sequestration [37].

Septic embolism

Meningococcal septicaemia can produce disseminated intravascular coagulation and tissue necrosis. Soft tissues are relatively easy to evaluate, but bone necrosis escapes clinical examination. This is a concern for the surgeon who has to decide the level of resection or amputation.

Bone scintigraphy significantly alters the management of limb surgery by demonstrating the level of bone viability, helping to avoid non-realistic limb reconstructions over necrotic bone areas [10].

Epiphyseal destruction and premature epiphyseal-metaphyseal fusion have also been described as late sequelae of bone infarction related to the septic embolism. Bone scintigraphy is able to detect these areas in the acute phase and has a prognostic value for future skeletal growing problems [38].

Skeletal trauma

Evaluation of fracture healing and bone fragment viability

Bone metabolism in children has a rapid turnover and this plays an important role in their particular response to trauma. The distinctive anatomy of the growing skeleton is also a clue to understanding traumatic injuries and reparative processes. Blood supply in long bones depends basically on the diaphyseal artery, which perfuses the diaphysis and the metaphysis. On the other hand, epiphyseal vascularisation is provided by small vessels related to the joint capsule. It is important to notice that the blood supply to the growing physeal cartilage is provided by epiphyseal vessels. Thus, any joint injury (trauma or infection) may affect both the epiphyseal ossification centre and the growth plate activity.

Bone loss, soft-tissue damage, compromised vascular supply and poor fracture fixation interfere with bone fracture healing, delaying consolidation, and possibly precluding normal bone union (non-union). Assessment of fracture healing by plain radiographs, CT or MRI can be difficult, especially with hardware in place. Bone scintigraphy lacks this limitation and has been used for the evaluation of bone fracture healing. There are two main types of non-union—hypertrophic or hypervascular and atrophic or avascular—and each one has unique findings in scintigraphy. In the hypertrophic type, bone fragments have rich osteoblastic activity showing increased blood flow, blood pool and radiotracer uptake

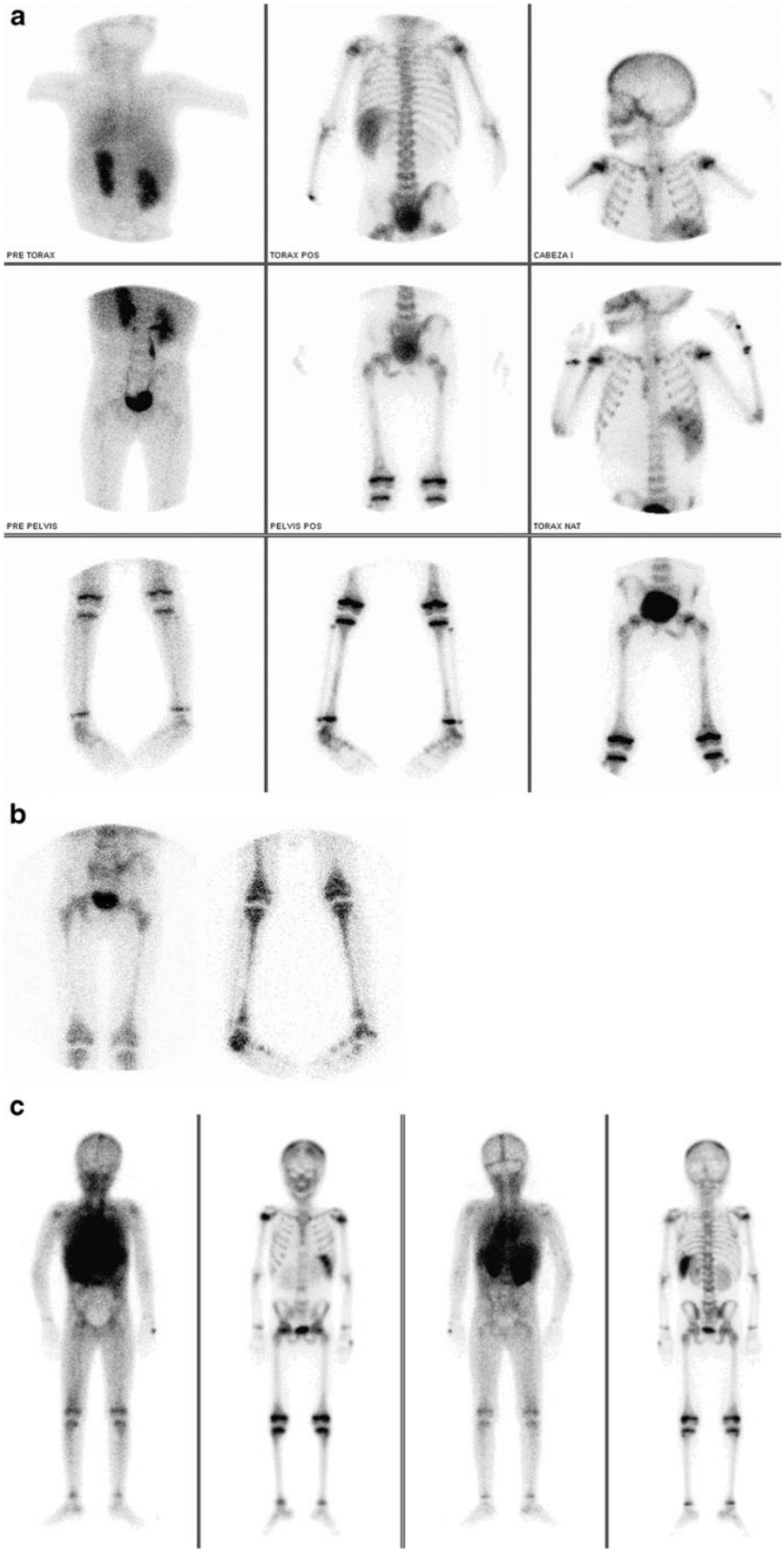

Fig. 4 Images in a 4-year-old girl with sickle cell disease and multiple episodes of bone pain since she was 3 months old. She had been admitted with fever and right pelvic and talus pain (normal radiograph, not shown). **a** Bone scintigraphy was performed, which showed cold areas in both iliac bones and an increased uptake of the right calcaneus. Other multiple bone uptake abnormalities are seen in femur and vertebrae. Related to the disease, an increased spleen uptake was also evident. **b** With suspicion of multiple bone infarcts and focal osteomyelitis, a ^{99m}Tc-white blood cell scan was indicated (images obtained 4 h after labelled white blood cell injection, **b**), detecting a focal leucocyte deposit on the right calcaneus. The image of the iliac bones is similar to the bone scan frame. The diagnosis of recent bone infarcts on both iliac bones and acute osteomyelitis on the right calcaneus was made and the girl was treated with IV antibiotics. **c** Two years later, the girl presented with pain on the right limb and the spine. Bone scintigraphy detected a recovery of normal bone uptake in iliac bones, but multiple cold areas in several spine vertebrae. Other focal abnormalities in bone uptake in multiple bones (skull, femur, calcaneus) were also evident. Findings were consistent with multiple new areas of bone infarct

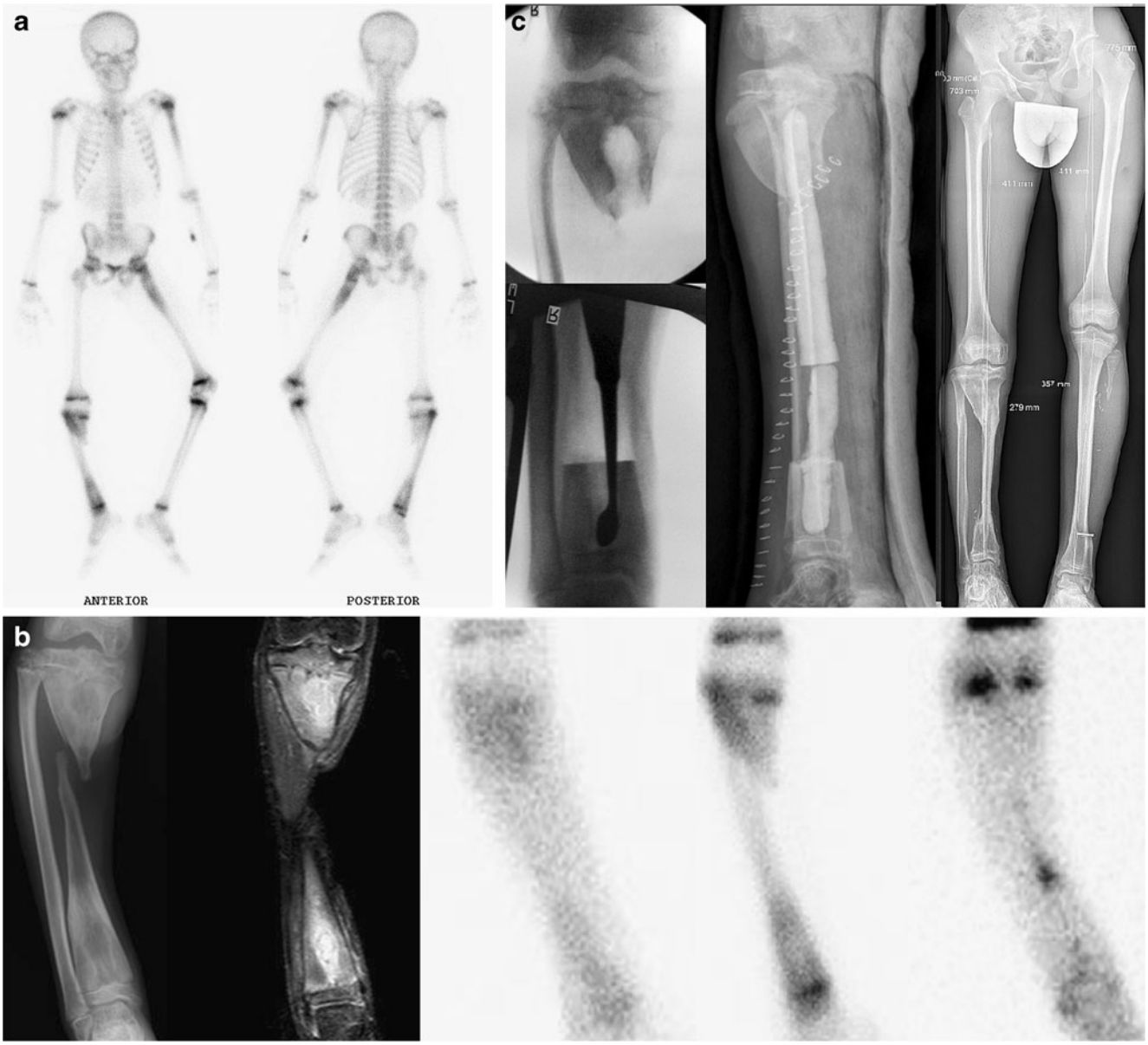

Fig. 5 A 9-year-old boy, living in a sub-Saharan country, presented with a 7-year history of chronic right tibia infection despite antibiotic treatment. Physical examination showed areas of scar and fistula in the leg and abnormal movement of the mid-tibia diaphysis. Radiography demonstrated tibia pseudoarthrosis and lucent medullar bone lesions with surrounding sclerosis in the proximal and distal tibia metaphysis suggesting sequestration. The clinical questions are whether there are other focuses of bone infection and if so, which is the activity of the infection. **a** A ^{99m}Tc whole-body bone scan shows multiple bone uptake foci in the left humerus, the left femur and the distal part of right tibia, with a cold area in the middle diaphysis. On the comparative imaging of the right tibia (**b** *from left to right*: radiograph, MRI, blood pool and delayed bone scan and ^{99m}Tc-labelled leucocyte), ^{99m}Tc-white blood cell scintigraphy detects an uptake in the middle diaphysis of the right tibia exclusively, suggesting septic activity at this point. Based on this information, surgery was performed consisting in right tibial diaphysis resection, metaphyseal curettage, cement and antibiotic. A vascularised fibular bone grafting was performed in a second stage (**c**). The other bone lesions responded to curettage and antibiotic treatment

in the bone-scan study. In these cases, the orthopaedic surgeon has to treat the fracture with a more stable fixation. In contrast, in the atrophic type of non-union, bone scan shows reduced bone-fragment blood flow, blood pool and radiotracer uptake, revealing impairment of normal osteoblastic activity.

FDG PET-CT imaging is an indicator of osteoblastic activity in vivo and has been used in experimental studies showing the ability to identify fracture non-unions at an early phase, not differentiating, however, metabolic activity between successful and delayed bone healing [39].

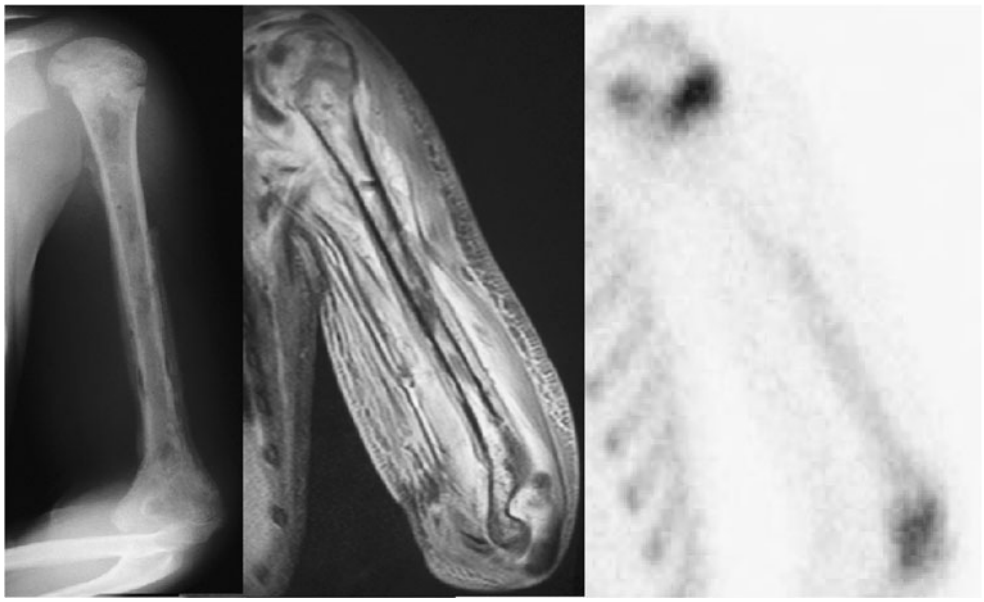

Fig. 6 Images in a 10-year-old girl with acute left proximal metaphyseal humeral osteomyelitis that progressed despite antibiotic treatment. Bone scan (*right*) demonstrates a cold area not only on the proximal part of the left humerus diaphysis but also a complete cold involvement of the humeral head. Radiograph (*left*) and MRI (*middle*) also demonstrated pandiaphysitis and involvement of the proximal epiphysis. MRI is superior to other techniques in demonstrating the joint involvement at the shoulder. The girl was treated surgically with debridement and sequestration resection. Sample culture was positive for MRSA and antibiotic treatment was finally successful. She ultimately developed focal humeral head collapse but recovered complete function, without pain

Physeal arrest

Growth disturbance of the long bones in children is frequently post-traumatic, but it also occurs because of physeal, epiphyseal or metaphyseal ischaemia. Regardless of the aetiology, physeal bridges may cause angular or longitudinal growth disturbances, depending on the site, extent and age of the patient.

In patients with at least 2 years or 2 cm of growth remaining, a resection of the bone bridge needs to be considered before the deformity is developed. Therefore, early recognition and mapping of the lesion is important.

Standard radiography can confirm the site and extent of the bony bridge in patients with obvious deformity, but problems of interpretation may arise if the deformity is not yet established or if the X-ray beam is not tangential to the physis. The physis of the distal femur and proximal tibia are the most frequently involved but they have a complex geometry making its evaluation difficult [40].

MRI exquisitely shows the growth disturbance and associated abnormalities that may follow physeal injury [41].

Scintigraphy can map the distribution of osteoblastic activity of the physis and is the only method that can distinguish between generalised growth slowdowns (Fig. 8) and complete epiphysiodesis [42]. Some authors have studied the normal tomoscintigraphic appearance of different physes and they suggest that bone scintigraphy allows to identify lesions greater than 1 cm [43].

Vascularised bone graft

Scintigraphy following vascularised bone transfer might be useful in several situations: postoperative vascular patency flap monitoring; assessment of unsuccessful bone graft union or hypertrophy; assessment of unsuccessful vascularised epiphyseal transfer remodelling; analysis of bone allograft revascularisation associated with vascularised periosteal flaps (Fig. 7).

A good correlation has been reported between blood supply and scintigraphy activity in vascularised free-flap transfer [44].

In the early postoperative phase, the surgeon needs an agile and repeatable tool to monitor flap vascularisation and eventually to perform a surgical revision of the vascular anastomosis if signs of flow interruption are shown (Fig. 8). Though scintigraphy could indirectly detect a vascular anastomosis problem, there are other methods (the implantable Doppler system, colour duplex US, near-infrared spectroscopy, micro dialysis laser Doppler flowmetry) more adequate for this purpose than scintigraphy [45]. On the contrary, in later phases of vascularised bone transfer, scintigraphy can be useful to discern whether a lack of bone hypertrophy or union is due to mechanical reasons or

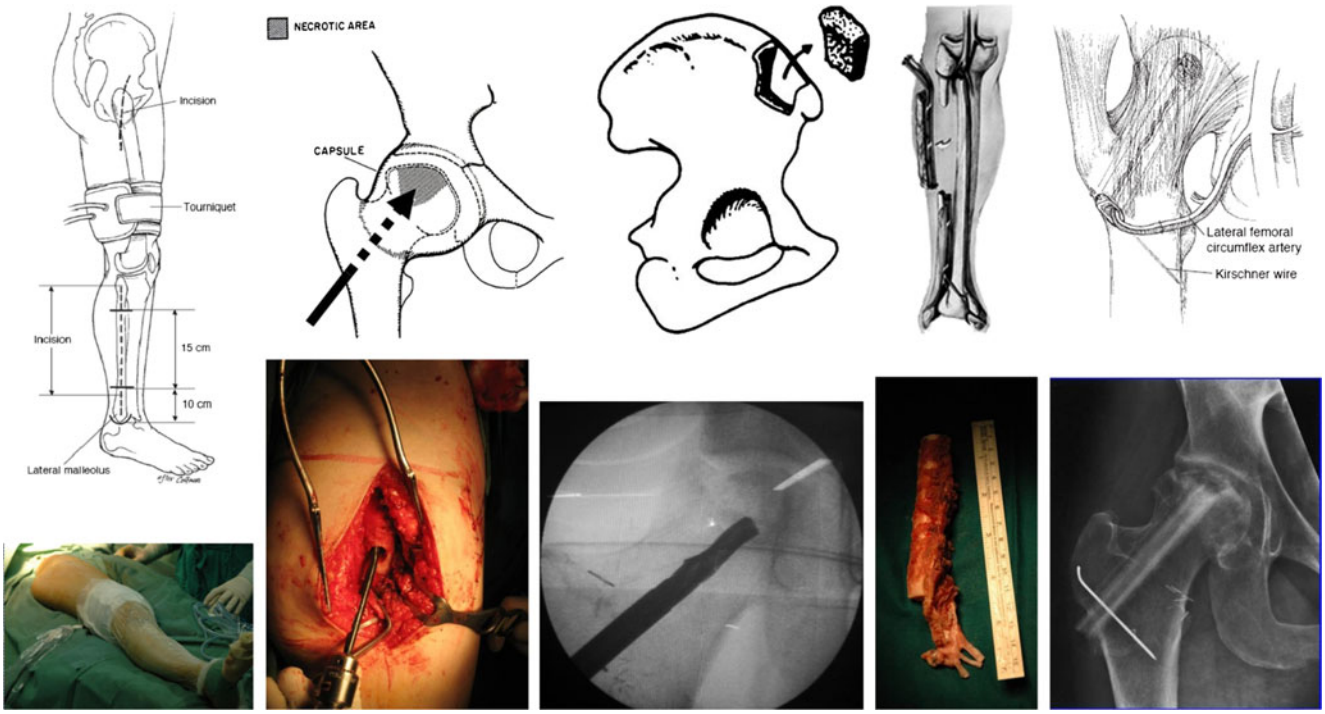

Fig. 7 Schematic representation (*top*) of vascularised peroneal graft surgery and corresponding images (*bottom*) of the technique. *From left to right*: Preparation for the double incision. Lateral femoral approach to reach the femoral head and remove necrotic bone. The gap is then filled with healthy bone from the iliac crest. Preparation of the free vascularised peroneal graft. Final position of the graft with its vascular anastomosis

to a lack of vascularisation in order to set up an adequate treatment.

Vascularised proximal fibular epiphyseal transplants are useful in the reconstruction of big joints after an epiphyseal tumour excision in very young children (<4–5 years old) [46]. At this age, implants or osteoarticular bone allografts are not indicated. In these grafts, the progressive physeal growth allows the generation of a new joint and avoids limb length discrepancy. Unfortunately, some of the vascularised epiphyseal transplants, although correctly vascularised, do not show remodelling. In these cases, (Fig. 9) scintigraphy is useful to ascertain whether lack of growth is due to an vascular patency problem or an intrinsecal physeal inactivity [47].

Massive bone allograft (MBA) is an inert and acellular structure used in limb reconstruction after bone tumour excision that does not revascularise over time even with the association of a vascularised fibular graft [48]. When a vascularised bone graft is associated, it enlarges over time but it is not able to revascularise the bone graft. Vascularised fibular periosteal graft (VFPG) has been recently described in children (Fig. 9) [49]. This flap, placed covering an MBA, is used after oncological bone tumour excision with an allograft revascularising purpose. In children, periosteum has a great osteogenic and vasculogenic power due to the presence of a high density of mesenchymal stem cells in the cambium layer. Although further experience and analysis is needed, studies by our group indicate that vascularised periosteal flaps might be able to revascularise massive bone allografts and scintigraphic studies are a good tool to monitor this phenomenon.

Points to take home

- Correlative anatomical and functional/metabolic imaging is the best diagnostic tool on offer.
- Bone scintigraphy is the reference standard for evaluating bone viability. The main clinical indications are for detection and follow-up of osteonecrosis, sequelae of infection and trauma septic embolism and, especially, vascularised bone graft viability.
- As always, the collaboration between clinicians, radiologists and nuclear medicine physicians is crucial. Feedback is necessary.
- Bone scan is critical for the detection and characterisation of osteonecrosis in an early phase when interventions may be most effective to ameliorate its progression. In addition, SPECT-CT has become a useful imaging tool to evaluate bone viability for

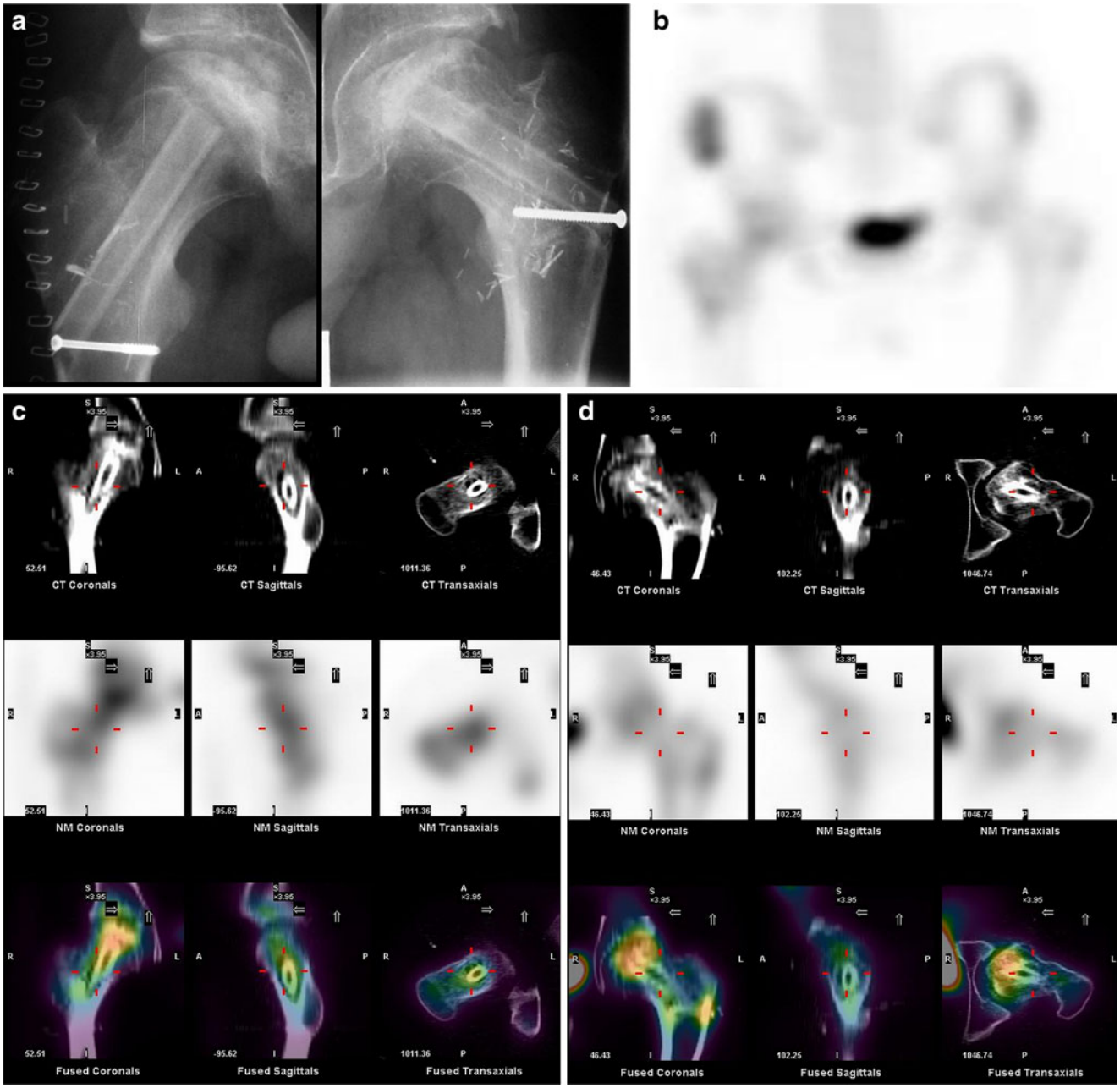

Fig. 8 Bone scintigraphy in vascularised bone graft in a 15-year-old boy with bilateral hip avascular necrosis treated with a synchronic vascularised bone graft surgery. Surgery was performed 6 months prior to imaging on the left hip and 15 days prior to imaging on the right hip. The clinical objectives at this point were to evaluate right hip bone graft viability and left hip re-perfusion induced by the bone graft. **a** AP radiograph of both hips shows correct positioning of the bone grafts. **b** Planar bone scans of the hips. Higher metabolic activity is seen in the right hip, where the surgery was more recent than on the left hip. Also bilateral mild hyperactivity on anterior iliac crest related to surgery can be appreciated (R>L). **c** SPECT-CT of the right hip. The highest activity is on the fibular graft. The femoral head is hypoactive, but not cold. **d** SPECT-CT left hip. The maximum metabolic activity is on the femoral head, indicating perfusion, bone viability and osteoblastic activity of the cancellous graft bone. The fibular cortex is isoactive

both graft and host in new surgical interventions using vascularised bone grafts.

- Changes on bone scintigraphy and pinhole imaging can identify the Conway patterns of early recanalisation or late neovascularisation, have an early prognostic value, and correlate with later radiographic Catterall and Herring classifications.
- Bone scintigraphy plays a role and has a prognostic value in evaluating limb reconstruction by demonstrating the level of bone viability.

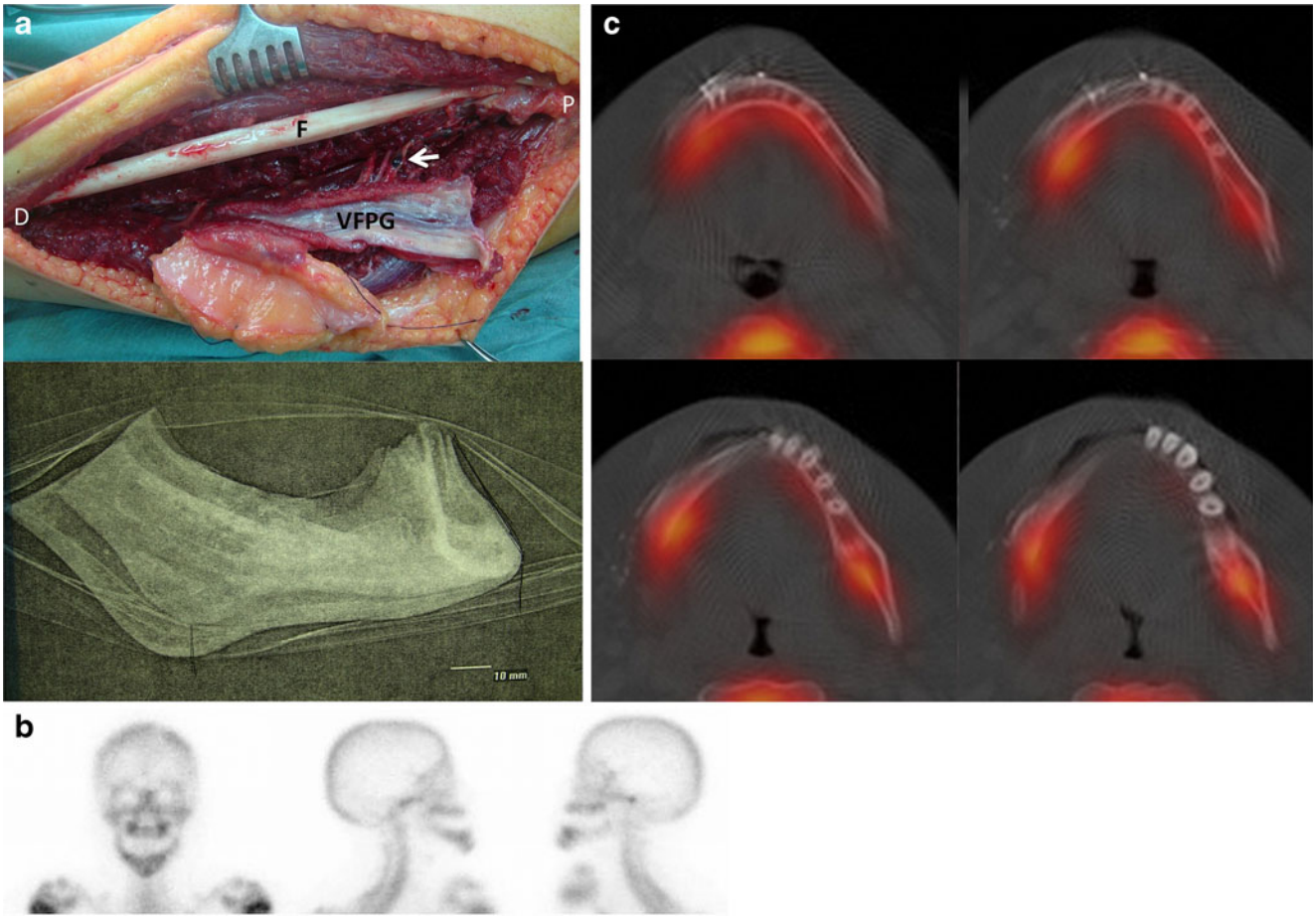

Fig. 9 Mandibular Ewing sarcoma in a 10-year-old girl. She had chemotherapy and surgery, consisting of block resection, structural cadaveric bone graft and fibular vascularised periostal graft. **a** An intraoperative picture shows the vascularised periosteal flap (*VFPG*), harvested from the left fibula (*F*) with a monitoring skin pad. The flap is still in situ before disconnection of the fibular vessels (*arrow*). The flap was then connected to the facial vessels and placed over the mandible allograft to revascularise it (*P* proximal, *D* distal). The radiograph corresponds to the mandible allograft that replaced the bone defect after the excision of a Ewing tumour. **b** Bone scan performed 12 months after surgery detects high bone graft uptake (higher than left mandibula), and SPECT-CT (**c**) shows good, uniform uptake in the graft, indicating excellent bone graft viability without necrotic or non-viable areas

- Bone scintigraphy has been used in the evaluation of fracture healing, differentiating between hypertrophic and atrophic non-union.
- Scintigraphy is a reliable tool for the evaluation of osteoblastic activity of the physis and it can identify growth disturbances before the deformity is present.
- Although scintigraphy is not the preferred tool for early monitoring of vascular patency in vascularised flaps, it is a useful technique to assess the cause of lack of vascularised bone graft hypertrophy or union and the lack of vascularised fibular epiphyseal transplant remodelling and to monitor the revascularisation of massive bone allograft by associated vascularised fibular periosteal grafts.

References

1. Moskowitz GW, Lukash F (1988) Evaluation of bone graft viability. Semin Nucl Med 18:246–254
2. Stevenson JS, Bright RW, Dunson GL et al (1974) Technetium-99m phosphate bone imaging: a method for assessing bone graft healing. Radiology 110:391–394
3. Lisbona R, Rosenthall L (1976) Assessment of bone viability by scintiscanning in frostbite injuries. J Trauma 16:989–992
4. Banzo J, Martínez Villén G, Abós MD et al (2002) Frostbite of the upper and lower limbs in an expert mountain climber: the value of bone scan in the prediction of amputation level. Rev Esp Med Nucl 21:366–369
5. Bhatnagar A, Sarker BB, Sawroop K et al (2002) Diagnosis, characterisation and evaluation of treatment response of frostbite using pertechnetate scintigraphy: a prospective study. Eur J Nucl Med Mol Imaging 29:170–175

6. Cauchy E, Chetaille E, Lefevre M et al (2000) The role of bone scanning in severe frostbite of the extremities: a retrospective study of 88 cases. Eur J Nucl Med 27:497–502
7. Salimi Z, Vas W, Tang-Barton P et al (1984) Assessment of tissue viability in frostbite by ^{99m}Tc pertechnetate scintigraphy. AJR Am J Roentgenol 142:415–419
8. Chang LY, Yang JY (1991) The role of bone scans in electric burns. Burns 17:250–253
9. Kao PF, Tzen KY, Huang MJ et al (1988) Using a gallium-67 scan to detect the extent of necrotizing fasciitis of the neck in diabetic ketoacidosis: report of a case. Taiwan Yi Xue Hui Za Zhi 87:224–227
10. Treharne LJ, Banwell P, Cadier M (2003) Mandatory bone scans for the assessment of extremity loss in meningococcal septicaemia? Br J Plast Surg 56:55–57
11. Lisbona R, Rennie WR, Daniel RK (1980) Radionuclide evaluation of free vascularized bone graft viability. AJR Am J Roentgenol 134:387–388
12. Velasco JG, Vega A, Leisorek A et al (1976) The early detection of free bone graft viability with ^{99m}Tc: a preliminary report. Br J Plast Surg 29:344–346
13. Conway JJ (1993) A scintigraphic classification of Legg-Calvé-Perthes disease. Semin Nucl Med 23:274–295
14. Rosovsky M, Goldfarb CR, Finestone H et al (1994) "Cold spots" in pediatric bone imaging. Semin Nucl Med 24:184–186
15. Harcke HT, Mandell GA (1993) Scintigraphic evaluation of the growth plate. Semin Nucl Med 23:266–273
16. Jones AG, Francis MD, Davis MA (1976) Bone scanning: radionuclidic reaction mechanisms. Semin Nucl Med 6:3–18
17. Grant FD, Fahey FH, Packard AB et al (2008) Skeletal PET with 18 F-fluoride: applying new technology to an old tracer. J Nucl Med 49:68–78
18. Blau M, Nagler W, Bender MA (1962) Fluorine-18: a new isotope for bone scanning. J Nucl Med 3:332–334
19. French RJ, McCready VR (1967) The use of 18-F for bone scanning. Br J Radiol 40:655–661
20. Stansfield EC, Sheehy N, Zurakowski D et al (2010) Pediatric ^{99m}Tc-MDP bone SPECT with ordered subset expectation. Radiology 257:793–801
21. Segall G, Delbeke D, Stabin MG et al (2010) SNM practice guideline for sodium 18f-fluoride PET/CT bone scans 1.0. J Nucl Med 51:1813–1820
22. Piepsz A, Hahn K, Roca I et al (1990) A radiopharmaceutical schedule for imaging in paediatrics. Eur J Nucl Med 17:127–129
23. Lassmann M, Biassoni L, Monsieurs M et al (2007) The new EANM paediatric dosage card. Eur J Nucl Med Mol Imaging 34:796–798
24. Lassmann M, Biassoni L, Monsieurs M et al (2008) The new EANM paediatric dosage card: additional notes with respect to F-18. Eur J Nucl Med Mol Imaging 35:1666–1668, Erratum in: Eur J Nucl Med Mol Imaging 35:2141
25. Sarikaya I, Sarikaya A, Holder LE (2001) The role of single photon emission computed tomography in bone imaging. Semin Nucl Med 31:3–16
26. Khoury J, Jerushalmi J, Loberant N et al (2007) Kohler disease: diagnoses and assessment by bone scintigraphy. Clin Nucl Med 32:179–181
27. Etchebehere EC, Etchebehere M, Gamba R et al (1998) Orthopedic pathology of the lower extremities: scintigraphic evaluation in the thigh, knee, and leg. Semin Nucl Med 28:41–61
28. Fragnière B, Chotel F, Vargas Barreto B et al (2001) The value of early postoperative bone scan in slipped capital femoral epiphysis. J Pediatr Orthop B 10:51–55
29. Brenner A, Koshy J, Mony J et al (2012) The bone scan. Semin Nucl Med 42:11–26
30. Comte F, De Rosa V, Zekri H (2003) Confirmation of the early prognostic value of bone scanning and pinhole imaging of the hip in Legg-Calvé-Perthes disease. J Nucl Med 44:1761–1766
31. Van Campenhout A, Moens P, Fabry G (2006) Serial bone scintigraphy in Legg-Calvé-Perthes disease: correlation with the Catterall and Herring classification. J Pediatr Orthop B 15:6–10
32. Lamer S, Dorgeret S, Khairouni A et al (2002) Femoral head vascularisation in Legg-Calvé-Perthes disease: comparison of dynamic gadolinium-enhanced subtraction MRI with bone scintigraphy. Pediatr Radiol 32:580–585
33. Dimeglio A, Canavese F (2011) Imaging in Legg-Calvé-Perthes disease. Orthop Clin North Am 42:297–302
34. Jaramillo D (2009) What is the optimal imaging of osteonecrosis, perthes, and bone infarcts? Pediatr Radiol 39(Suppl 2): S216–S219
35. Ejindu VC, Hine AL, Mashayekhi M et al (2007) Musculoskeletal manifestations of sickle cell disease. Radiographics 27:1005–1021
36. Nadel HR (2007) Bone scan update. Semin Nucl Med 37:332–339
37. Squire KR, Fessler JF, Blevins WE et al (1990) Full-length diaphyseal sequestrum as a consequence of segmental transverse fractures of the large metatarsal bone in a calf. J Am Vet Med Assoc 196:2006–2008
38. Duncan JS, Ramsay LE (1984) Widespread bone infarction complicating meningococcal septicaemia and disseminated intravascular coagulation. Br Med J (Clin Res Ed) 288:111–112
39. Hsu WK, Feeley BT, Krenek L et al (2007) The use of 18f-fluoride and 18 F-FDG PET scans to assess fracture healing in a rat femur model. Eur J Nucl Med Mol Imaging 34:1291–1301
40. Ecklund K, Jaramillo D (2001) Imaging of growth disturbance in children. Radiol Clin North Am 39:823–841
41. Ecklund K, Jaramillo D (2002) Patterns of premature physeal arrest: MR imaging of 111 children. AJR Am J Roentgenol 178:967–972
42. Khoshhal KI, Kiefer GN (2005) Physeal bridge resection. J Am Acad Orthop Surg 13:47–58
43. Yang KT, Yang AD (2006) Evaluation of activity of epiphyseal plates in growing males and females. Calcif Tissue Int 78:348–356
44. Schrey A, Niemi T, Kinnunen I et al (2010) The limitations of tissue-oxygen measurement and positron emission tomography as additional methods for postoperative breast reconstruction free-flap monitoring. J Plast Reconstr Aesthet Surg 63:314–321
45. Smit JM, Zeebregts CJ, Acosta R (2010) Advancements in free flap monitoring in the last decade: a critical review. Plast Reconstr Surg 125:177–185
46. Innocenti M, Delcroix L, Romano GF et al (2007) Vascularized epiphyseal transplant. Orthop Clin North Am 38:95–101, vii
47. Soldado F, Fontecha CG, Haddad S et al (2012) Composite vascularized fibular epiphyseo-osteo-periosteal transfer for hip reconstruction after proximal femoral tumoral resection in a 4-year-old child. Microsurgery 32:489–492
48. Capanna R, Campanacci DA, Belot N et al (2007) A new reconstructive technique for intercalary defects of long bones: the association of massive allograft with vascularized fibular autograft. Long-term results and comparison with alternative techniques. Orthop Clin North Am 238:51–60
49. Soldado F, Fontecha CG, Barber I et al (2012) Vascularized fibular periosteal graft: a new technique to enhance bone union in children. J Pediatr Orthop 32:308–313